doi: 10.15407/ujpe61.06.0495

M.S. BRODYN,[1] S.A. MULENKO,[2] V.I. RUDENKO,[1] V.R. LIAKHOVETSKYI,[1] M.V. VOLOVYK,[1] N. STEFAN [3]

[1] Institute of Physics, Nat. Acad. of Sci. of Ukraine
(46, Prosp. Nauky, Kyiv 03680, Ukraine)
[2] G.V. Kurdyumov Institute for Metal Physics, Nat. Acad. of Sci. of Ukraine
(36, Vernadskyi Ave., Kyiv 03142, Ukraine)
[3] National Institute for Laser, Plasma and Radiation Physics
(PO Box MG-54, Magurele RO-77125, Romania)

PACS 42.70.Mp, 78.20.-e, 81.15.Fg

CUBIC OPTICAL NONLINEARITY OF THIN Fe_2O_3 AND Cr_2O_3 FILMS SYNTHESIZED BY PULSED LASER DEPOSITION

The extinction spectra and the parameters of cubic optical nonlinearity in thin Fe_2O_3 and Cr_2O_3 films deposited on glass substrates with the use of the laser sputtering method have been measured. The cubic optical nonlinearity is studied, by using femtosecond laser radiation with the wavelength $\lambda = 800$ nm and the pulse duration $\tau = 180$ fs. The energy gap width evaluated from the extinction spectra is found to equal $E_g \approx 2.4$ eV and 2.2 eV for Fe_2O_3 films synthesized on the substrates at temperatures of 293 K and 800 K, respectively, and $E_g \approx 3$ eV for Cr_2O_3 films deposited on the substrate heated up to 800 K. Rather high values are obtained for the coefficients of refractive nonlinearity: $Re\chi^{(3)} \sim 10^{-6}$ esu for Fe_2O_3 films and $Re\chi^{(3)} \sim 10^{-7}$ esu for Cr_2O_3 ones. The determined values of $Im\chi^{(3)}$ amounted to about $10^{-6}\div10^{-7}$ esu for Fe_2O_3 films and about 10^{-8} esu for Cr_2O_3 ones. Probable mechanisms of refractive nonlinearity have been proposed.

Keywords: cubic optical nonlinearity, thin Fe_2O_3 and Cr_2O_3 films, laser sputtering method, femtosecond laser radiation.

1. Introduction

The search for nonlinear optical media with a high cubic nonlinearity and a high operation rate of this nonlinearity remains an important problem for needs of modern optoelectronics. Recently, it has been demonstrated in a number of works [1–6] that low-dimensional structures (thin films, nanoparticle composites) of transition metal oxides, in particular, Fe_2O_3, are characterized by rather a high refractive nonlinearity and represent a considerable practical interest. For instance, in work [1], the coefficient of cubic nonlinear susceptibility $\chi^{(3)} = 2 \times 10^{-9}$ esu was obtained at the laser wavelength $\lambda = 480$ nm and the laser pulse duration $\tau = 180$ fs for amorphous Fe_2O_3 films fabricated, by using the sol-gel method. For crystalline α-Fe_2O_3 and γ-Fe_2O_3 films synthesized within the same method, the $\chi^{(3)}$-values obtained under the nanosecond laser radiation with $\lambda = 1.9$ μm and $\tau = 10$ ns were 5.8×10^{-11} esu and 2.1×10^{-11} esu, respectively [3]. In work [6], the value $\chi^{(3)} = 5 \times 10^{-6}$ esu was obtained for Fe_2O_3 films fabricated using the laser ablation method and picosecond laser radiation ($\lambda = 532$ nm, $\tau = 30$ ps).

The available data testify that the magnitude of cubic nonlinearity in Fe_2O_3 films depends substantially on the film manufacturing methods, film structure, and parameters of laser radiation used at measurements. Therefore, it seems important to obtain data concerning the nonlinear optical response of Fe_2O_3 films grown up with the use of the pulsed laser sputtering method, when laser pulses of femtosecond duration are applied.

Fe_2O_3 is a semiconductor with the energy gap width $E_g = 2.2$ eV [7]. It is transparent in the visible spectral range. With the aim in view to find a nonlinear optical material with a wider transparency window, we also considered chromium oxide (Cr_2O_3) with the energy gap width $E_g = 3.4$ eV [8]. This is

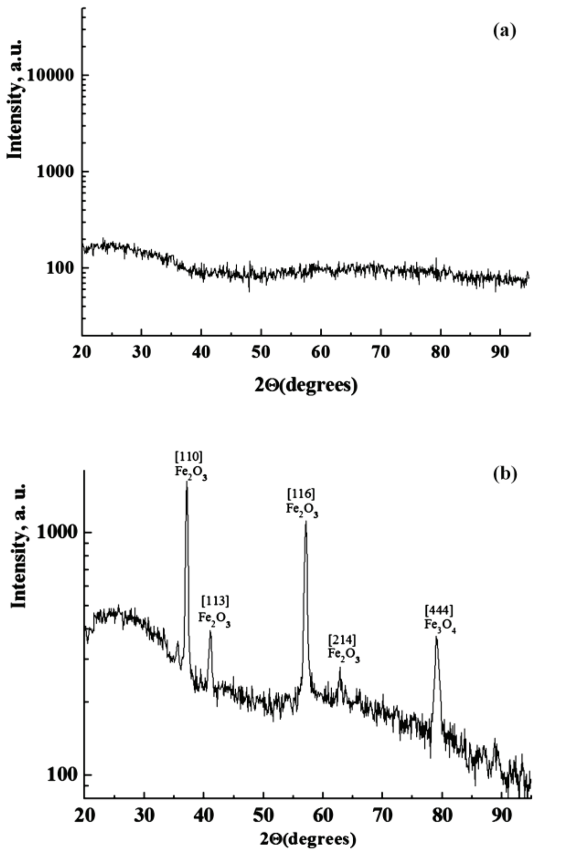

Fig. 1. XRD patterns of nano-scale Fe_2O_{3-x} films deposited, by using the reactive laser deposition method on SiO_2 substrates: at $T_s = 293$ K and $P_{O_2} = 0.1$ Pa, (*a*) and at $T_s = 800$ K and $P_{O_2} = 0.1$ Pa (*b*)

a material that is promising for the creation of selective absorbing films for the solar energy conversion and so on [9]. In earlier works, linear optical and spectral properties of thin Cr_2O_3 films fabricated by, in particular, the chemical vapor deposition [10] and chemical pyrolysis sputtering [11] techniques showed that the spectrum shape depends to some extent on the method of film fabrication. However, the nonlinear optical properties of Cr_2O_3 films, unlike those of Fe_2O_3 ones, have not been studied enough. In particular, we did not manage to find works dealing with the cubic optical nonlinearity in Cr_2O_3 films, although the theoretical [12] and experimental [13] researches of the quadratic nonlinearity (the second harmonic generation) are known.

In this work, with the help of femtosecond laser radiation ($\lambda = 800$ nm, $\tau = 180$ fs), the coefficient of cubic susceptibility $\chi^{(3)}$ was measured in amorphous and crystalline Fe_2O_3 and Cr_2O_3 films synthesized by the pulsed laser sputtering at various substrate temperatures and various oxygen pressures in a vacuum chamber. Possible mechanisms of cubic nonlinearity in the examined films are analyzed.

2. Experimental Part

2.1. Sample fabrication

Nano-sized films of iron and chromium oxides were synthesized using the method of reactive pulsed laser deposition onto SiO_2 substrates. The deposition was carried out in a vacuum reactor made of stainless steel. In order to avoid the contamination, the vacuum chamber was pumped out to a residual pressure of about 4.5×10^{-5} Pa before every deposition. Pure oxygen (99.999%) was let into the chamber until its dynamic pressure became stabilized at values of 0.1, 0.5, or 1.0 Pa. Pure Fe (99.5%) was knocked out from a target with the help of radiation emitted by a KrF ($\lambda = 248$ nm) pulsed excimer laser with an energy density of 4.0 J/cm^2, a pulse repetition frequency of 10 Hz, and a pulse duration of about 25 ns. Every film was deposited by applying a definite number of laser pulses (4000, 5000, and 6000, respectively) corresponding to the oxygen pressure in the reactor. In order to avoid the breakdown and to provide the ablation process smoothness, the target was rotated at a rotation frequency of 3 Hz. Before each deposition, the target surface was cleaned, making use of 3000 laser pulses, provided that the substrate was closed.

The flux of knocked out iron ions was gathered on the SiO_2 substrate, which had been cleaned in an ultrasonic bath with ethanol and deionized by water. The substrate was arranged in parallel to the target and at a distance of 45 mm from the latter. The thickness of deposited films was measured with the help of a profilometer "Tensor Instruments", the model "Alpha-step 100", with an error of 5%. The X-ray diffraction (XRD) analysis of Fe_2O_3 films was carried out with the help of an X-ray diffractometer "Stoe" at 45 kW and 33 mA (Cu K_α radiation). The corresponding results showed that the films deposited on the SiO_2 substrate at room temperature ($T_s = 293$ K) had an amorphous structure, whereas the films deposited on the same substrate but heated up to the temperature $T_s = 800$ K had a polycrystalline structure. This can be seen in Fig. 1, where the XRD patterns for those two film types are exhibited.

The results of our researches showed that the films, which were obtained at a higher oxygen pressure, contained a larger amount of oxidized iron or chromium than the samples deposited at a lower pressure. Moreover, the higher the oxygen pressure, the thinner was the film deposited on the SiO_2 substrate, by using the same number of laser pulses.

It should be noted that polycrystalline films, besides the main Fe_2O_3 phase, also included a small amount of Fe_3O_4 phase with the energy gap width $E_g = 0.1$ eV [14]. Unfortunately, the X-ray diffraction analysis of Cr_2O_3 films was not done.

2.2. Experimental technique of optical researches

Extinction spectra in the interval from 300 to 1100 nm were measured with the help of a monochromator MDR-6. The absorption coefficient of the sample was calculated using the formula

$$\alpha = \frac{1}{L} \ln \frac{(1-R)^2}{T}, \quad (1)$$

where T is the sample transmittance, L the sample thickness, and R the reflectance from the sample surface, which was evaluated on the basis of the refractive index: $n_0 = 2.75$ for Fe_2O_3 and $n_0 = 2.5$ for Cr_2O_3 [15].

The research of optical nonlinearity was carried out with the help of the known Z-scan technique [16]. The scheme of experimental installation is shown in Fig. 2. In our experiment, we used a titanium-doped sapphire laser with the generation wavelength $\lambda = 800$ nm, a pulse repetition frequency of 75 MHz, and the pulse duration $\tau = 180$ fs. The laser beam was focused by a lens with a focal length of 35 cm. The beam waist diameter in various cases amounted to 36 or 29 μm. The laser beam intensity at the focus, I_0, was 0.3 and 0.9 GW/cm^2, respectively, and the aperture transmittance S was equal to 0.169 and 0.121, respectively.

The coefficient of refractive index nonlinearity, n_2, and the real part of cubic nonlinear susceptibility, Re$\chi^{(3)}$, were calculated, by using the data obtained for the normalized transmittance in the scheme of Z-scan experiment with the closed aperture (CA), by the well-known expressions [16, 17]

$$n_2 = \frac{\Delta T_{p-v}\lambda}{0.406(1-S)^{0.27} 2\pi I_0 L_{\text{eff}}}, \quad (2)$$

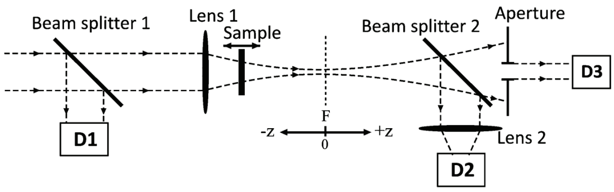

Fig. 2. Schematic diagram of the experimental installation for measuring the parameters of cubic nonlinearity

$$\text{Re}\,\chi^{(3)}\,(\text{esu}) = \frac{3n_0^2 n_2}{160\pi^2}\,(\text{m}^2\text{W}^{-1}), \quad (3)$$

where ΔT_{p-v} is the normalized difference between the transmittance maximum and minimum in the CA scheme, S the aperture transmittance (the fraction of radiation that reached a photodiode), I_0 the light intensity at the focus point, n_0 the linear refractive index, and $L_{\text{eff}} = [1 - \exp(-\alpha L)]/\alpha$ is the effective length of the sample.

In the case of the scheme with the open aperture (OA), the coefficient of nonlinear absorption β was calculated on the basis of the following approximation for the obtained normalized transmittance data [14]:

$$T(z) = -\frac{q_0}{2\sqrt{2}} \frac{1}{[1 + z^2/z_0^2]} \quad \text{at} \quad |q_0| \ll 1, \quad (4)$$

where $q_0(z) = \beta I_0 L_{\text{eff}}$.

The imaginary part of the coefficient of third-order nonlinear susceptibility, Im$\chi^{(3)}$, is related to the coefficient of nonlinear absorption β by the relation [16]

$$\text{Im}\,\chi^{(3)}\,(\text{esu}) = \frac{c^2 n_0^2 \beta}{240\pi^2\omega}\,(\text{mW}^{-1}), \quad (5)$$

where ω is the light field frequency.

3. Results and Their Discussion

3.1. Extinction spectra

The extinction spectra of the examined Fe_2O_3 films synthesized at various oxygen pressures in the chamber (0.1, 0.5, and 1 Pa) are depicted in Fig. 3. Panel *a* corresponds to amorphous films obtained on the substrate with the temperature $T_s = 293$ K, and panel *b* to polycrystalline films obtained on the substrate heated to the temperature $T_s = 800$ K.

From Fig. 3, *a*, one can see that the shape of extinction curves for the studied films changes rather substantially from sample to sample. The extinction curve of the amorphous film obtained at an oxygen

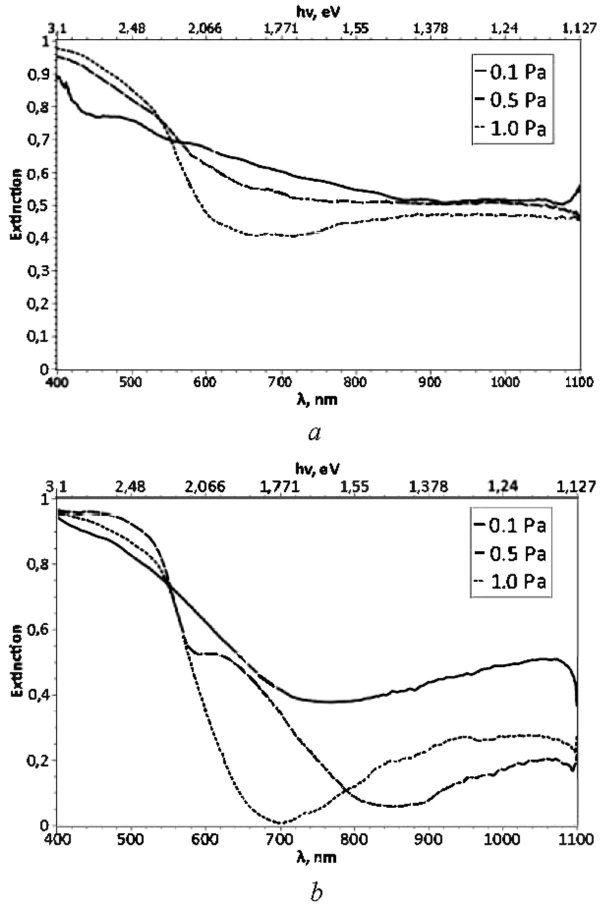

Fig. 3. Extinction spectra of amorphous Fe_2O_3 films (a) and polycrystalline Fe_2O_3 films (b) synthesized at various oxygen pressures in a reactor

pressure of 0.1 Pa demonstrates a smooth recession of absorption from shorter to longer wavelengths with no distinctly pronounced edge. In the curve corresponding to the amorphous film obtained at an oxygen pressure of 0.5 Pa, one can see a shoulder in the wavelength interval of 520–680 nm. For the film obtained at an oxygen pressure of 1 Pa, this shoulder becomes rather sharp and located in the interval of 520–600 nm. This shoulder testifies to the presence of quasiforbidden gap in the films concerned. Being estimated by the shoulder shape, the width of this gap, E'_g , was found to equal approximately 2.4 eV, which is close to the energy gap width in α-Fe_2O_3 [7].

Hence, the amorphous films can be considered as semiconductors with characteristic tails of the density of states near the edges of the valence and conduction bands, and with a set of various local levels in the quasiforbidden gap. The shape of extinction curves confirms this conclusion. In the interval of 900–1000 nm, an extinction plateau is observed at approximately the same, rather high, level for all three films.

The extinction curves for polycrystalline films (Fig. 3, b) changed their shape considerably. The absorption edge became sharper, especially for the film grown at the maximum oxygen pressure of 1 Pa. Moreover, it is a little shifted toward long waves in comparison with the amorphous sample spectrum. Attention is attracted by the appearance of rather a pronounced "hump" at $\lambda \approx 630$ nm in the spectrum of the film obtained at an oxygen pressure of 0.5 Pa, and the presence of deep and wide valleys in the spectra of the films synthesized at oxygen pressures of 0.5 ($\lambda \approx 700$ nm) and 1 Pa ($\lambda \approx 830$ nm).

As was marked above (see Fig. 1, b), the polycrystalline Fe_2O_3 films fabricated at the oxygen pressure in a chamber $P_{O_2} = 0.1$ Pa contained the crystalline phase Fe_3O_4. This fact explains the higher absorption and the spectrum structure in the interval of 700–1100 nm (the intrinsic absorption range for Fe_3O_4) for this specimen and is confirmed by the absorption spectra of Fe_3O_4 films measured in work [3].

We also studied Cr_2O_3 films deposited on glass substrates. One of them was deposited at a temperature of 293 K and a pressure of 0.5 Pa in a chamber. Two others were deposited on substrates heated up to a temperature of 800 K and at an oxygen pressure of 0.1 or 0.5 Pa in a chamber. By analogy with Fe_2O_3, we may assume that the film deposited at a substrate temperature of 293 K is amorphous, and those deposited at a substrate temperature of 800 K are polycrystalline. The extinctions curves measured for those films in the interval of 380–1100 nm are shown in Fig. 4.

From Fig. 4, one can see that the spectra of all three films had a more or less sloping edge in the interval of 400–450 nm. The edge is the sharpest for the film deposited at a substrate temperature of 800 K and the oxygen pressure $P_{O_2} = 0.1$ Pa. The films deposited at $P_{O_2} = 0.5$ Pa had more extended edges. The value of E_g determined from the shape of absorption edge for the film deposited at an oxygen pressure of 0.1 Pa in the sputtering chamber was found to equal 3 eV. In the spectral interval of 500–1100 nm, there is a considerable damping background with appreciable maxima at 600 and 940 nm, which are most likely associated with extrinsic absorption.

3.2. Nonlinear optical properties

3.2.1. Fe_2O_3

Nonlinear optical parameters were measured for two groups of Fe_2O_3 thin film samples. One of them included the films deposited on the substrate at a temperature of 293 K and oxygen pressures of 0.1, 0.5, and 1 Pa in a chamber. The other group included the films deposited on the substrate heated to a temperature of 800 K and at the same oxygen pressures in a chamber. As was mentioned above, the films in the former group had an amorphous structure, and those in the latter group a polycrystalline one. In Fig. 5, the dependences of the normalized transmittance of the Fe_2O_3 film deposited at $T_s = 293$ K and $P_{O_2} = 1$ Pa on its Z-position with respect to the focus (the Z-scan scheme) are exhibited. These dependences were used to determine the parameters of cubic nonlinearity: $\mathrm{Re}\chi^{(3)}$, $\mathrm{Im}\chi^{(3)}$, n_2, and β. The corresponding values obtained for the analyzed Fe_2O_3 films are listed in Table 1. In the table, T_s is the substrate temperature, P_{O_2} the oxygen pressure in the chamber, L the sample thickness, and I_0 the light intensity at the lens focus.

From Table 1, one can see that, for the amorphous films that were fabricated at oxygen pressures of 0.5 and 1 Pa, the values of $\mathrm{Re}\chi^{(3)}$ turned out by an order of magnitude larger than their counterparts for the polycrystalline films. The values of $\mathrm{Re}\chi^{(3)}$ are positive for all samples. The maximum value of the real part of cubic nonlinear susceptibility, $\mathrm{Re}\chi^{(3)} = 6.45 \times 10^{-6}$ esu, was obtained for the amorphous film deposited at an oxygen pressure of 0.5 Pa in a chamber.

Table 1 also contains the coefficients of nonlinear absorption β. The lowest β-value was obtained for the amorphous film synthesized at an oxygen pressure of 0.5 Pa. The $\mathrm{Re}\chi^{(3)}$-value for this sample turned out the largest.

We would like to make the following remark concerning the probable origin of refractive nonlinearity. It is known [18] that the positive refractive nonlinearity in semiconductors can be connected with the nonlinear polarization of bound electrons (the Kerr nonlinearity) or with the processes of intraband scattering of equilibrium electrons under the influence of intensive light radiation. With regard for the shape of extinction curves, namely, rather a high absorption background and the smeared edge of intrinsic absorption, it is possible to assume the presence of various impurity levels in the energy gap, in particular, near the conduction band bottom, and, hence, the presence of a considerable concentration of equilibrium electrons thermally excited at room temperature, at which the nonlinear optical measurements were carried out. Rather a high dark conductivity of the film also testifies to this assumption. Therefore, it is highly probable that the refractive nonlinearity of

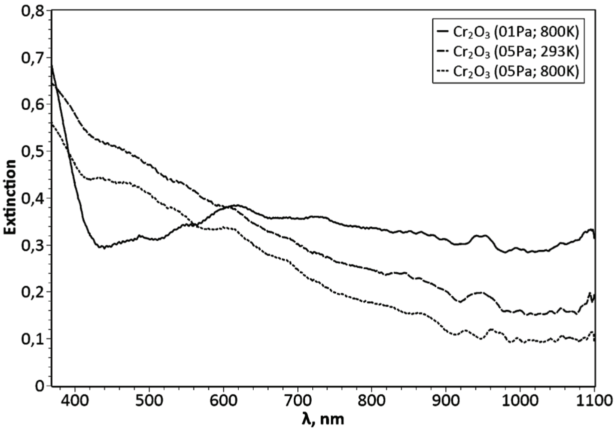

Fig. 4. Extinction spectra of amorphous and polycrystalline Cr_2O_3 films synthesized at various oxygen pressures in the reactor

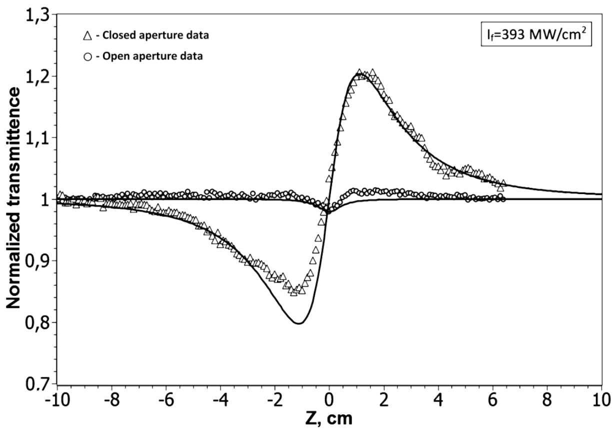

Fig. 5. Z-scan dependences of the normalized transmittance of the Fe_2O_3 film deposited at $T_s = 293$ K and an oxygen pressure of 1 Pa on the film position Z with respect to the focus in the femtosecond experiment ($\lambda = 800$ nm). The solid curve demonstrates the corresponding theoretical approximation

Table 1. **Nonlinear optical parameters of examined Fe_2O_3 films**

Sample	T_s, K	P_{O_2}, Pa	L, μm	α, cm^{-1}	I_0, GW/cm^2	n_2, cm^2/W	β, cm/W	Re$\chi^{(3)}$, esu	Im$\chi^{(3)}$, esu
Fe_2O_3	293	0.1	0.053	1.826×10^5	0.393	4.541×10^{-9}	2.433×10^{-5}	6.524×10^{-7}	2.965×10^{-8}
Fe_2O_3	293	0.5	0.026	3.429×10^5	0.393	4.491×10^{-8}	1.433×10^{-4}	6.453×10^{-6}	1.747×10^{-7}
Fe_2O_3	293	1.0	0.013	5.808×10^5	0.393	3.288×10^{-8}	1.671×10^{-4}	4.724×10^{-6}	2.037×10^{-7}
Fe_2O_3	800	0.1	0.06	1.09×10^5	0.866	5.826×10^{-9}	2.623×10^{-5}	8.37×10^{-7}	3.197×10^{-8}
Fe_2O_3	800	0.5	0.045	0.441×10^5	0.866	3.97×10^{-9}	2.434×10^{-4}	5.704×10^{-7}	2.967×10^{-7}
Fe_2O_3	800	1.0	0.04	1.001×10^5	0.351	3.195×10^{-8}	3.461×10^{-5}	4.59×10^{-7}	4.218×10^{-8}

Table 2. **Nonlinear optical parameters of examined Cr_2O_3 films**

Sample	T_s, K	P_{O_2}, Pa	L, μm	α, cm^{-1}	I_0, GW/cm^2	n_2, cm^2/W	β, cm/W	Re$\chi^{(3)}$, esu	Im$\chi^{(3)}$, esu
Cr_2O_3	800	0.1	0.07	7.232×10^4	0.866	6.283×10^{-10}	7.993×10^{-6}	7.46×10^{-8}	8.05×10^{-9}
Cr_2O_3	293	0.5	0.055	8.595×10^4	0.866	1.472×10^{-9}	-1.371×10^{-5}	1.748×10^{-7}	-1.381×10^{-8}
Cr_2O_3	800	0.5	0.07	5.891×10^4	0.866	1.04×10^{-9}	2.578×10^{-5}	1.235×10^{-7}	2.597×10^{-8}

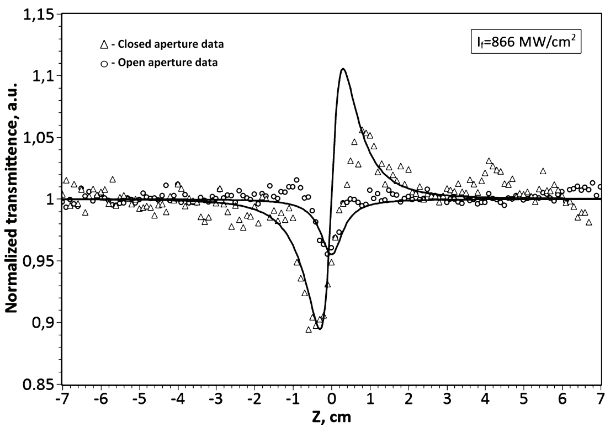

Fig. 6. The same as in Fig. 5, but for the Cr_2O_3 film deposited at $T_s = 800$ K and an oxygen pressure of 0.5 Pa

researched films is associated, to a great extent, with the processes of intraband scattering of equilibrium charge carriers, if the non-parabolic character of the conduction band is taken into account and owing to the dependence of the relaxation time of electrons in the band on their energy. In this case, the "Kerr" nonlinearity may also make a contribution to the value of Re$\chi^{(3)}$.

3.2.2. Cr_2O_3

In Fig. 6, the dependence of the normalized transmittance of a Cr_2O_3 film on the Z-position of the film with respect to the focus in the Z-scan scheme measured at the substrate temperature $T_s = 800$ K and an oxygen pressure of 0.5 Pa is shown. Table 2 contains the corresponding values of nonlinear optical parameters for the examined Cr_2O_3 films at $\lambda = 800$ nm determined form the Z-scan curves. The notations are the same as in Table 1.

One can see that the refractive nonlinearity Re$\chi^{(3)}$ is positive for all samples, i.e. self-focusing takes place. The maximum value Re$\chi^{(3)} = 1.75 \times 10^{-7}$ esu was obtained for the amorphous film deposited at an oxygen pressure of 0.5 Pa. The values of Re$\chi^{(3)}$ for the polycrystalline films deposited at oxygen pressures of 0.1 and 0.5 Pa were of the same order, but 2.2 and 1.4, respectively, times lower than the maximum. By comparing those values with the data obtained for the Fe_2O_3 films, we see that they are approximately an order of magnitude smaller.

Analogously to the case of Fe_2O_3 films, the refractive nonlinearity in the Cr_2O_3 ones can be connected with the cumulative contribution made by the processes of intraband scattering of free equilibrium electrons and nonlinear polarization of bound electrons. Taking into account that the wavelength of an applied laser was 800 nm, the shift from the absorption edge is much larger in the Cr_2O_3 case. Therefore, the contribution of the nonlinear polarization of bound electrons in Cr_2O_3 can be smaller than in Fe_2O_3.

4. Conclusions

With the help of the Z-scan method and making use of laser radiation ($\lambda = 800$ nm, $\tau = 180$ fs), the parameters of cubic optical nonlinearity were measured in thin (nano-sized) Fe_2O_3 and Cr_2O_3 films deposited on glass substrates using the laser ablation technique. Depending on the substrate temperature at the sputtering, T_s, the Fe_2O_3 and Cr_2O_3 films had either an amorphous ($T_s = 293$ K) or polycrystalline ($T_s = 800$ K) structure. The energy gap width E_g evaluated from the extinction spectra was found to equal $E_g \approx 2.4$ eV and $E_g \approx 2.2$ eV for Fe_2O_3 films synthesized on the substrates at temperatures 293 and 800 K, respectively, and $E_g \approx 3$ eV for Cr_2O_3 films deposited on the substrate heated to 800 K. The coefficient of cubic nonlinear susceptibility $\mathrm{Re}\chi^{(3)}$ was determined to be of an order of 10^{-6} or 10^{-7} esu for Fe_2O_3 films with the amorphous or polycrystalline structure, respectively. The largest value $\mathrm{Re}\chi^{(3)} = 6.45 \times 10^{-6}$ esu was obtained for the amorphous Fe_2O_3 film deposited at an oxygen pressure of 0.5 Pa in the sputtering chamber. All iron oxide films revealed a nonlinear absorption with the coefficient β of about 10^{-4}–10^{-5} cm/W. At the same time, the Cr_2O_3 films obtained at $T_s = 800$ K showed a nonlinear absorption with $\beta \sim 10^{-5}$ cm/W, whereas the Cr_2O_3 films sputtered at $T_s = 293$ K demonstrated a nonlinear enlightenment. The most probable mechanisms of refractive nonlinearities in all studied specimens seem to be the "Kerr" nonlinearity and the intraband scattering of equilibrium electrons under the influence of laser radiation. Rather high values of refractive non-linearity in the examined film materials make them promising for practical applications in optoelectronic devices.

The work was performed on a laser installation of the Laser Femtosecond Center of the NAS of Ukraine at the Institute of Physics. The authors are grateful to the employees of the Center for the assistance at measurements.

1. H.S. Zhou, A. Mito, D. Kundu, and I. Honma, J. Sol-Gel Sci. Techn. **19**, 539 (2000).
2. T. Hashimoto, T. Yoko, and S. Sakka, J. Ceram. Soc. Jpn. **101**, 64 (1993).
3. T. Hashimoto, T. Yamada, and T. Yoko, J. Appl. Phys. **80**, 3184 (1996).
4. B. Yu, C. Zhu, and F. Gan, Physica E **8**, 360 (2000).
5. G. Chatzikyriakos, K. Iliopoulos, A. Bakandritsos, and S. Couris, Chem. Phys. Lett. **493**, 314 (2010).
6. S.A. Mulenko, M.S. Brodyn, and V.Ya. Gayvoronsky, Proc. SPIE **6161**, 616107 (2006).
7. H. Jiang, R.I. Gomez-Abal, P. Rinke, and M. Scheffler, Phys. Rev. B **82**, 045108 (2009).
8. J.A. Crawford and R.W. Vest, J. Appl. Phys. **35**, 2413 (1964).
9. S. Sahoo and C. Binek, Phil. Mag. Lett. **87**, 3 (2007).
10. Chun-Shen Cheng, H. Gomi, and H. Sakat, Phys. Status Solidi A **155**, 417 (1996).
11. Z.T. Khodair, G.A. Kazem, and A.A. Habeeb, Iraqi J. Phys. **10**, 17 (2012).
12. V.N. Muthukumar, R. Valentí, and C. Gros, Phys. Rev. B **54**, 433 (1996).
13. R.V. Pisarev, M. Fiebig, and D. Fröhlich, Ferroelectrics **204**, 1 (1997).
14. L. Blaney, Lehigh Rev. **15**, 5 (2007).
15. R. Shannon, R. Shannon, O. Medenbach, and R. Fischer, J. Phys. Chem. Ref. Data **31**, 4 (2002).
16. M. Sheik-Bahae, A.A. Said, T.H. Wei, D.J. Hagan, and E.W. Van Stryland, IEEE J. Quantum Elect. **26**, 760 (1990).
17. H.M. Gibbs, *Optical Bistability: Controlling Light with Light* (Academic Press, New York, 1985).
18. A.A. Borshch, M.S. Brodin, and V.I. Volkov, *Refractive Nonlinearity of Wide-Band Semiconductors and Applications* (Harwood Academic Publ., Chur, 1990).

Received 19.01.16.

Translated from Ukrainian by O.I. Voitenko

М.С. Бродин, С.А. Муленко, В.І. Руденко, В.Р. Ляховецький, М.В. Воловик, Н. Стефан

ОПТИЧНА КУБІЧНА НЕЛІНІЙНІСТЬ ТОНКИХ ПЛІВОК Fe_2O_3 І Cr_2O_3, СИНТЕЗОВАНИХ МЕТОДОМ ІМПУЛЬСНОГО ЛАЗЕРНОГО ОСАДЖЕННЯ

Р е з ю м е

Проведено вимірювання спектрів екстинкції та параметрів оптичної кубічної нелінійності тонких плівок Fe_2O_3 та Cr_2O_3, осаджених на скляні підкладки методом імпульсного лазерного напилення. Дослідження оптичної кубічної нелінійності проводилось з використанням фемтосекундного випромінювання на довжині хвилі $\lambda = 800$ нм з тривалістю імпульсів $\tau = 180$ фс. Оцінені за спектрами екстинкції ширини заборонених зон дорівнюють, відповідно, $E_g \sim 2{,}4$ еВ і 2,2 еВ для плівок Fe_2O_3, синтезованих на підкладки при температурах 293 К і 800 К та $E_g \sim 3$ еВ для плівок Cr_2O_3, осаджених на підкладку, нагріту до 800 К. Отримано досить високі значення коефіцієнтів рефрактивної нелінійності $\mathrm{Re}\chi^{(3)} \sim 10^{-6}$ esu для плівок Fe_2O_3 і $\mathrm{Re}\chi^{(3)} \sim 10^{-7}$ esu для плівок Cr_2O_3. Визначені величини $\mathrm{Im}\chi^{(3)}$ становили по порядку для Fe_2O_3 – 10^{-6}–10^{-7} esu, а для плівок Cr_2O_3 – 10^{-8} esu. Запропоновані можливі механізми рефрактивної нелінійності.